

# Detecting the orbital motion of nearby supermassive black hole binaries with *Gaia*

Daniel J. D’Orazio\* and Abraham Loeb

*Department of Astronomy, Harvard University, 60 Garden Street Cambridge, Massachusetts 01238, USA*



(Received 7 September 2018; published 20 November 2019)

We show that a 10-yr *Gaia* mission could astrometrically detect the orbital motion of  $\sim 1$  subparsec separation supermassive black hole binary in the heart of nearby, bright active galactic nuclei (AGN). Candidate AGN lie out to a redshift of  $z = 0.02$  and in the V-band magnitude range  $10 \lesssim m_V \lesssim 13$ . The distribution of detectable binary masses peaks at a few times  $\sim 10^7 M_\odot$  and is truncated above a few times  $\sim 10^8 M_\odot$ .

DOI: [10.1103/PhysRevD.100.103016](https://doi.org/10.1103/PhysRevD.100.103016)

## I. INTRODUCTION

The *Gaia* satellite is mapping the positions of the stars with unprecedented precision. Its 5-yr mission: to survey the six-dimensional phase space coordinates of a billion stars to an astrometric precision of a few  $\mu\text{as}$  [1–3]. *Gaia* will observe not only stars, but all optical sources brighter than an apparent magnitude of  $\sim 20$ . This includes active galactic nuclei (AGN), namely distant and powerful sources of multiwavelength emission driven by gas accretion onto supermassive black holes (SBHs) at the centers of galaxies.

AGN are used to calibrate *Gaia* astrometric position measurements, both via *Gaia*’s optical astrometry as well as with radio-frequency VLBI [4]. The AGN are chosen as calibrators because they are distant and hence expected to exhibit very little proper motion or parallax. Despite this expectation, *Gaia* has detected  $\gtrsim 1$  mas offsets in optical and radio positions of AGN, probing dislodged AGN or radio/optical jet properties [5–8]. In this paper, we show that on  $\lesssim 50 \mu\text{as}$  scales, this expectation is also relevant for AGN that harbor subparsec (pc) separation SBH binaries (SBHBs). Orbital motion of one or both accreting SBHs in an SBHB can change the position of the optical emitting region of the AGN by an angle greater than the astrometric precision of *Gaia*. SBHB orbital motion would be distinct from the linear motion expected for a jet or ejected AGN. Because binary-induced motions will only occur for a minority of AGN, there will be little impact on *Gaia*’s calibration. This observation does, however, present a path toward definitive detections of sub-pc separation SBHBs.

While solid lines of evidence lead us to expect that SBHBs reside in the centers of some galaxies [9], their definitive detection at sub-pc separations is yet to be obtained. The existence of sub-pc SBHBs is of special importance as it embodies the “final-parsec problem”

[9,10], determining the fate of SBHBs. If interaction with the environments in galactic nuclei can drive SBHBs to sub-pc separations, then they will merge via emission of gravitational waves (GWs), detectable out to redshifts  $z \gtrsim 10$  by the future space-based GW observatory LISA [11], and generating a low-frequency stochastic GW background detectable by the pulsar timing arrays (PTAs) [12].

To determine which, if any, proposed mechanisms, [e.g., [13–18]], solve the final-parsec problem in nature, one must characterize a population of sub-pc SBHBs. Current detection methods are indirect and require campaigns that last many years [e.g., [19–48]]. While these techniques provide a way toward identifying and vetting SBHB candidates via a combination of indirect methods, a more direct approach is desired.

Recently, we have shown that mm-wavelength VLBI possesses the astrometric resolution and longevity to repeatedly image SBHB orbits out to redshift  $z \sim 0.5$ , providing direct evidence for SBHBs in radio-loud AGN [49]. The technique that we propose here also directly tracks the SBHB orbit with the advantage that target AGN need not be bright in mm-wavelengths and that unlike VLBI, *Gaia* is conducting a survey mission that will map the entire sky, and, as we show, could find evidence for SBHBs within the next 5–10 yr.

## II. HOW MANY SBHBs COULD GAIA DETECT?

The angular scale of nearby sub-pc separation SBHBs is  $\mathcal{O}(10) \mu\text{as}$ . The diffraction-limited imaging resolution of *Gaia* is  $\sim 10^4$  times larger. While *Gaia* cannot image sub-pc separation SBHBs, it does possess the astrometric precision to detect  $\sim 10 \mu\text{as}$  centroid shifts in bright sources.

We consider the case where only one SBH in the SBHB is luminous [e.g., Ref. [50]]. Over the course of an orbit, the position of the SBH, and thus the center of light, changes by a characteristic value given by the semimajor axis of the

\*daniel.dorazio@cfa.harvard.edu

binary,  $a$  (see Sec. III B for further discussion). At angular-diameter distance  $D_A(z)$ , the orbital angular extent is  $\theta_{\text{orb}} \approx a/D_A(z)$ . *Gaia* can detect orbital motion if  $\theta_{\text{orb}}$  is greater than its astrometric precision, and if the orbital period is shorter than twice the mission lifetime.

*Gaia*’s astrometric resolution can be parametrized by the brightness and color of the source. Working in Johnson V-band magnitudes, we adopt an average AGN  $V - I_c = 0.7$  based on the  $r - i$  colors of nearby ( $z \leq 2.1$ ) SDSS AGN [51], and color correction equations [52], that yield a  $V - I_c$  range of 0.3–1.1. We use the fitting formula from Eqs. (4) to (7) of Ref. [2] and the *Gaia* G-band to V-band conversion [53] to compute the V-band magnitude-dependent astrometric resolution of *Gaia*. The astrometric end-of-mission resolution,  $\sigma_{\text{eom}}$ , is  $9 \mu\text{s}$  for a  $m_V = 13$  AGN [4]. This corresponds to a physical separation of  $\sim 0.01$  pc at a distance of 200 Mpc, suggesting that *Gaia* can probe sub-pc, GW-driven SBHBs if they reside in nearby bright AGN.

Multiple works have considered exoplanet detection with *Gaia* [54–58]. We draw on this body of work which shows that the relevant quantity to consider for astrometric orbital detection is the signal-to-noise ratio,  $\text{SNR} = \theta_{\text{orb}}/\sigma_{\text{single}}$ , where  $\sigma_{\text{single}}$  is the precision for a single scan which we compute as  $\sigma_{\text{single}} = \sqrt{70}/(2.15 \times 1.2)\sigma_{\text{eom}}$ , the 5-yr end-of-mission astrometric precision multiplied by the sky-position-averaged number of scans per source (over 5 yr) and geometric sky averaging factors [57]. As shown in Ref. [58], an SNR of 2.3 (1.7) is required to achieve a % 50 detection rate for a 5-yr (10-yr) *Gaia* mission, with a false-positive rate estimated at  $\lesssim 10^{-4}$ . Hence, in this work, we adopt a minimum  $\text{SNR} = 2$  corresponding to a minimum detectable orbital angular size of  $\theta_{\text{min}} = 2\sigma_{\text{single}}$ . Next we compute the expected number of such *Gaia*-detectable SBHBs for both a 5-yr mission and an extended 10-yr mission.

### A. Calculation

We use the quasar luminosity function [QLF; [59]] to derive the number of AGN per redshift  $z$  and luminosity  $L$ . From  $L$  and  $z$ , and a bolometric correction to the V-band of 10 [60], we find the corresponding V-band magnitude  $m_V(L, z)$ , which gives the astrometric resolution,  $\theta_{\text{min}}$ . Combined with the redshift, this yields the minimum binary separation that *Gaia* can detect in that luminosity and redshift bin. At each luminosity bin we derive a total binary mass from the assumption that the AGN emits at a fraction of Eddington luminosity,  $L = f_{\text{Edd}}L_{\text{Edd}}(M)$ . The minimum binary separation and the binary mass yield the minimum binary orbital period for which *Gaia* could detect orbital motion,

$$P_{\text{min}}(L, z) = \frac{2\pi[\theta_{\text{min}}(L, z)D_A(z)]^{3/2}}{\sqrt{GM(L, f_{\text{Edd}})}}. \quad (1)$$

We adopt  $f_{\text{Edd}} = 0.1$ , motivated by an average value for bright AGN [61,62].

We additionally require that the binary complete at least one orbit over the course of the *Gaia* mission. Otherwise orbital motion is difficult to detect [58] or could be confused with linear motion. The combined requirements constrain  $P_{\text{min}}(L, z)$  to be less than a maximum time period  $P_{\text{max}} = 10$  yr (5 yr) for a 10-yr (5-yr) *Gaia* mission. We call AGN for which  $P_{\text{min}}(L, z) \leq P_{\text{max}}$  “*Gaia* targets.” This estimate, however, does not account for the probability that an AGN harbors an SBHB at the desired orbital period. To estimate this, we assume that a fraction  $f_{\text{bin}}$  of all AGN are triggered by SBHBs. We then use the quasar lifetime  $t_Q$  and the residence time of an SBHB at orbital period  $P$  to compute the fraction of  $t_Q$  that a binary spends at orbital periods below  $P$  [see, e.g., [29,49]]. The residence time due to GW emission is

$$t_{\text{res}} \equiv \frac{a}{\dot{a}} = \frac{20}{256} \left(\frac{P}{2\pi}\right)^{8/3} \left(\frac{GM}{c^3}\right)^{-5/3} q_s^{-1} \quad (2)$$

for binary symmetric mass ratio  $q_s \equiv 4q/(1+q)^2$ , where  $q \equiv M_2/M_1 \leq 1$  and  $M_1 + M_2 = M$ . The probability for observing the binary at orbital periods  $\leq P$  is given by  $\mathcal{F}(P, M, q_s) = \text{Min}[t_{\text{res}}(P, M, q_s)/t_Q, 1]$ . We evaluate the residence time at  $P_{\text{min}}$ .

The total number of *Gaia*-detectable SBHBs is

$$N_{\text{SBHB}} = f_{\text{bin}} \int_0^\infty \left\{ 4\pi \frac{d^2V}{dzd\Omega} \int_{\log L_{\text{min}}(z)}^\infty \frac{d^2N}{d \log L dV} \mathcal{F}(P, M, q_s) \times \mathcal{H}[P_{\text{max}} - P_{\text{min}}(L, z)] \right\} d \log L dz, \quad (3)$$

where  $d^2N/d \log L dV$  is the pure-luminosity-evolution, double-power-law QLF with redshift dependent slopes from Ref. [59] (last row of Table 3 labeled “Full”).  $d^2V/dz d\Omega$  is the comoving volume per redshift and solid angle [63],  $\mathcal{H}$  denotes the Heaviside function,  $m_V(L_{\text{min}}, z) = 21$ , and we choose a fiducial quasar lifetime  $t_Q = 10^7$  yr [49,64].

### B. Results

Table I lists parameter choices and the resulting total number of *Gaia*-detectable SBHBs. For fiducial values, and a 10-yr *Gaia* mission,  $N_{\text{SBHB}} \approx 11f_{\text{bin}}$ . Thus, if the fraction of SBHBs in local bright AGN is  $f_{\text{bin}} \gtrsim 0.1$ , *Gaia* has the potential to find an SBHB during an extended, 10-yr lifetime. Previous studies have argued for a similar value of  $f_{\text{bin}}$  (typically 10%, which is our fiducial value) based upon periodic variability searches in AGN [31,34].

Table I also lists our “optimistic” and “pessimistic” parameter choices. In the optimistic case,  $N_{\text{SBHB}} \approx 13f_{\text{bin}}$

TABLE I. Model parameters and the resulting number of *Gaia*-detectable SBHBs (note that a 20-yr mission lifetime requires a successor to *Gaia*).

Parameter	Meaning	Fiducial	Optimistic	Pessimistic
$f_{\text{bin}}$	The fraction of AGN harboring SBHBs	0.1	"	"
$f_{\text{Edd}}$	The Eddington fraction of bright AGN	0.1	"	"
$BC$	Bolometric correction from V-band	10.0	"	"
$t_Q$	The AGN lifetime	$10^7$ yr	$5 \times 10^6$ yr	$10^8$ yr
$V - I_c$	A mean color for nearby AGN	0.7	1.1	0.0
$P_{\text{max}}$	Mission lifetime	10 yrs (5 yr) (20 yr)	10 yr (5 yr) (20 yr)	10 yr (5 yr) (20 yr)
$q$	Binary mass ratio	0.1	0.05	1.0
$N_{\text{SBHB}}$	Number of detectable ( $\text{SNR} \geq 2$ ) SBHBs	<b>1.1</b> (0.3) (3.1)	<b>1.3</b> (0.4) (3.8)	<b>0.8</b> (0.2) (2.0)

SBHBs. In the pessimistic case,  $N_{\text{SBHB}} \approx 8f_{\text{bin}}$  SBHBs. For each case, we also consider the benefit of 20 yr of observation (while *Gaia* cannot last that long, another 10 yr of a successor mission could fulfill this in the future [e.g., Ref. [65]]). Such an extended mission could result in up to  $38f_{\text{bin}}$  putative SMBHB detections.

Figure 1 plots distributions of *Gaia* SBHB candidates vs V-band magnitude, redshift, and binary mass. We show (i) the total number of AGN found from integrating the QLF (black-dotted line); (ii) the number of “*Gaia*-target” AGN, (teal-dashed line); (iii) “binary-targets,” including the probability  $\mathcal{F}(M, P, q_s)$  for an AGN to contain a binary at the desired orbital period (orange line); and (iv) the binary-targets with  $\text{SNR} \geq 2$ , for which  $\geq 50\%$  of the population will be detectable with a  $\lesssim 10^{-4}$  false-positive rate. The teal and solid-orange lines (ii and iii) are drawn for  $\text{SNR} \geq 1$  in order to more easily discuss the target population discussed below and to compare to the  $\text{SNR} \geq 2$  case. Integration under the dashed-orange lines and multiplication by  $f_{\text{bin}}$  yields  $N_{\text{SBHB}}$  in Table I. For reference, the gray histograms show the observed distribution of nearby AGN with  $m_V < 16$  [66]. Note, however, that magnitudes relevant for our study are those of the central point source,

presumably generated by accretion onto either component of a putative binary, whereas magnitudes from Véron-Cetty and Véron [66] can include also the extended host galaxy for such nearby systems. Hence, the Véron-Cetty and Véron [66] catalog may overestimate the number of nearby bright systems in the context of this work.

The left panel of Fig. 1 displays the number of SBHBs per AGN V-band magnitude. Comparing the teal-dashed line labeled “*Gaia* target” and the black-dotted line (all AGN), we see that the orbital period cut  $P_{\text{min}} \leq P_{\text{max}}$  removes AGN with  $m_V \gtrsim 12.5$ . This is because *Gaia*’s resolution worsens for dimmer targets. To illustrate this, the purple dot-dashed line plotted on the right vertical axis of the left panel shows *Gaia*’s single-scan astrometric precision vs  $m_V$ .

Comparison of the dashed-teal line with the solid-orange line shows that brighter AGN in the “*Gaia* target” distribution is less likely to harbor an SBHB at the required orbital period  $P_{\text{min}}$ . This is because nearby, bright AGN correspond to more luminous AGN which correspond to AGN with higher binary masses via the Eddington relation. At a fixed orbital period, higher mass binaries inspiral more quickly and are hence less likely to be found. Where the

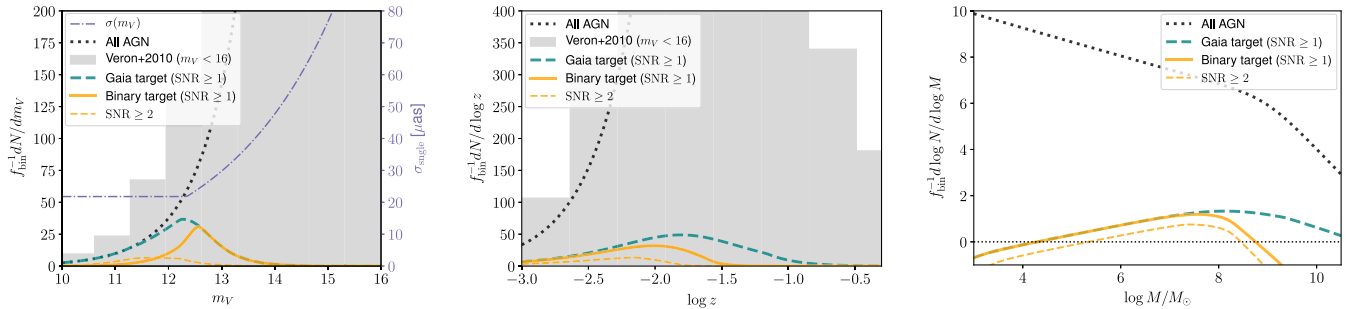


FIG. 1. The number of AGN per V-band magnitude (left), log redshift (middle), and log binary mass (right) for four different populations. The dashed-black line shows all AGN. The teal-dashed line, labeled “*Gaia*-target” shows only the AGN for which the minimum *Gaia*-resolvable binary orbital period [Eq. (1)] is shorter than a 10-yr *Gaia* lifetime. The orange lines weight the *Gaia*-target distribution by the probability for finding an SBHB at the required orbital period (with  $f_{\text{bin}} = 1$  and  $\text{SNR} = 1$  for visualization). The dashed-orange lines show only those binaries with a  $\geq 50\%$  detection rate ( $\text{SNR} \geq 2$ ). The gray histograms count known AGN with  $m_V \leq 16.0$  [66]. In the left panel, the purple dot-dashed line and corresponding right-vertical axis show the single-scan astrometric precision of *Gaia*.

teal and orange curves overlap is where the binary residence time is at least the quasar lifetime.

The dashed-orange line for  $\text{SNR} \geq 2$  binaries effectively represents a population with a larger minimum orbital period. Hence, there are fewer such binaries that lie between this minimum and  $P_{\text{max}}$ . The dashed-orange line is higher than the solid-orange line at bright magnitudes because the probability  $\mathcal{F}$  is larger due to a longer minimum orbital period. The dashed-orange line shows that for the fiducial case, the detectable SBHB distribution peaks at  $m_V = 12$ , with an expectation value greater than  $1f_{\text{bin}}$  for AGN with  $10.3 \leq m_V \leq 13$ .

The middle panel of Fig. 1 displays the redshift distribution of *Gaia*-detectable SBHBs. The maximum-orbital-period cut removes candidate AGN at all redshifts, while the binary-target distribution is reduced in number from the *Gaia*-target distribution at higher redshifts. The latter is because SBHBs at higher redshift must be more luminous in order for *Gaia* to resolve orbital motion. Again, more luminous AGN are associated with more massive SBHBs which merge more quickly. The  $\text{SNR} \geq 2$  binaries (dashed-orange line) have a  $\log z$  distribution peaking at  $z \sim 0.01$  with expectation value  $\geq 1f_{\text{bin}}$  for  $z \leq 0.02$ .

The right panel of Fig. 1 displays the distribution in binary mass of *Gaia*-detectable SBHBs. Comparison of the black-dotted and teal-dashed lines shows that the highest fraction of AGN are removed from the *Gaia*-target distribution at lower binary masses. This is because SBHBs with lower masses have much longer orbital periods for the same angular separation and redshift. Again, the comparison of the solid-orange and teal-dashed lines shows that the expectation value for the number of *Gaia*-detectable SBHBs also decreases for more massive binaries. For fiducial parameter values, the  $\text{SNR} \geq 2$  binaries distribute in  $\log M$  with a peak at  $M \sim 3 \times 10^7$  and expectation value  $\geq 1f_{\text{bin}}$  for  $M \leq 3 \times 10^8 M_\odot$ .

For optimistic (pessimistic) parameter values (Table I), the distributions peak at nearly the same magnitudes with a similar though slightly increased (decreased) range, and extends to higher (lower) redshifts  $z \lesssim 0.02$  ( $z \lesssim 0.01$ ), and higher (lower) binary masses  $M \lesssim 5 \times 10^8 M_\odot$  ( $M \lesssim 8 \times 10^7 M_\odot$ ). For a shorter, 5-yr mission lifetime, the  $\text{SNR} \geq 2$  population peaks at a slightly dimmer  $m_V \sim 11$  and has expectation value  $\geq 1f_{\text{bin}}$  for  $10.4 \leq m_V \leq 12$ ,  $z \leq 0.01$ , and  $M \leq 4 \times 10^7 M_\odot$ .

Cumulative distributions of  $\text{SNR} \geq 2$  binary targets in orbital period and orbital velocity are plotted in Fig. 2. The period distribution (blue) shows the fraction of *Gaia*-detectable SBHBs as a function of  $P_{\text{max}}$ . We note that, while we assume a constant 5-yr mission-end resolution, this may change over the course of a longer mission due to better point spread function fitting, but also due to possible instrument degradation. The linear dependence of the period distribution indicates that the period restriction

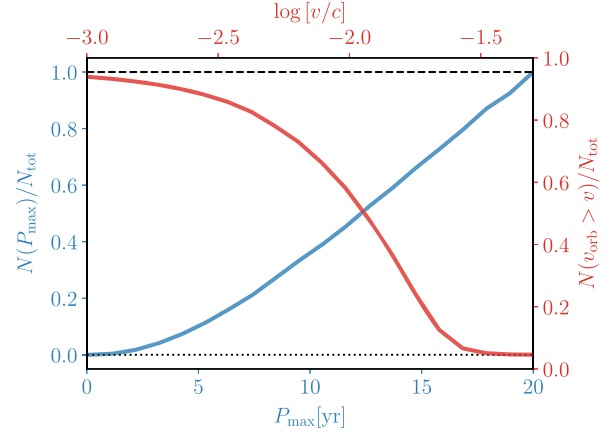


FIG. 2. *Blue curve and left-bottom axes:* the fraction of *Gaia*-detectable binaries vs maximum detectable orbital period  $P_{\text{max}}$  (for a total number referenced to  $P_{\text{max}} = 20$  yr). *Red curve and right-top axes:* the fraction of *Gaia*-detectable binaries with orbital velocity of the secondary (mass ratio of 0.1) greater than the labeled x-axis value. The orbital velocity in units of the speed of light approximates the amplitude of modulations induced by the orbital Doppler boost.

$P_{\text{min}} < P_{\text{max}}$  dominates over the steeper  $t_{\text{res}} \propto P^{8/3}$  residence-time dependence.

The velocity distribution (red) shows the number of *Gaia*-detectable SBHBs with orbital velocity  $v_{\text{orb}}/c$  above velocity  $v/c$ . This quantity sets the fractional amplitude of photometric modulations caused by the relativistic Doppler boost, given by  $\Delta F_\nu/F_\nu \approx (3 - \alpha_\nu)v_{\text{orb}}/c \cos I$ , for specific flux  $F_\nu$ ,  $v_{\text{orb}}/c \ll 1$ , inclination of the orbital plane to the line of sight  $I$ , and frequency-dependent spectral slope  $\alpha_\nu$  (with typical values  $-2 \lesssim \alpha_\nu \lesssim 2$ ) (see Refs. [50,67]). We compute  $v_{\text{orb}}/c$  as that of the secondary with  $q = 0.1$ .

Figure 2 shows that *Gaia*-detectable SBHBs will have  $v_{\text{orb}}/c \lesssim 0.03$ . Hence, for  $\alpha_\nu = -2$ , Doppler-induced modulations will have  $\Delta F_\nu/F_\nu \leq 5\%$ , translating to  $\Delta m_V \leq 0.05$  mag amplitude modulations. *Gaia*’s photometric precision is better than 0.01 mag at  $m_V \lesssim 14$  [3,68] and could identify Doppler modulation coincident with astrometric shifts of AGN optical regions. However, at  $\sim$ year timescales, intrinsic AGN variability has often a higher amplitude than the maximum  $\Delta m_V = 0.05$  mag Doppler signal predicted here [69], and finding this signal without a *Gaia* detection would be difficult. If *Gaia* identifies an SBHB candidate and its orbital period astrometrically, then a targeted search for periodicity at the identified orbital period, as well as further photometric monitoring beyond the lifespan of *Gaia*, could identify Doppler modulations, further validating the SBHB interpretation.

### III. DISCUSSION

Binary motion can be uniquely identified and disentangled from linear motion. Orbital motion in AGN would not be mistaken for a stellar binary because of the much



shorter orbital periods associated with more massive SBHs at the measured orbital separation. Moreover, *Gaia* measures high-resolution spectra of objects with  $V \leq 15.5$  [2], implying that AGN can be identified unambiguously. Additionally, because *Gaia* will observe each bright object on the sky a median of 72 times (for the 5-yr mission) [2], candidate AGN spectra could be monitored for broad-line variations hypothesized to accompany SBHBs [e.g., [28]], though *Gaia*'s spectral resolution may not be sufficient to detect such broad-line shifts and variations. Broad-line monitoring from *Gaia* or ground-based spectroscopic measurements along with multiwavelength photometric monitoring for binary-induced periodicity [e.g., [31,34–36,50,70]] could be used in tandem with *Gaia* orbital tracking to prove the existence of sub-pc separation SBHBs, and build an SBHB identification ladder by studying the characteristics of confirmed SBHB-harboring AGN.

Because we predict the *Gaia*-detectable SBHBs to lie in nearby, bright AGN, future work should examine these known sources. Those exhibiting, e.g., periodic variability should be given priority for examination in the *Gaia* dataset. If any *Gaia* SBHB candidates are radio-loud, they can be targeted by mm-VLBI observatories that could simultaneously track the orbital motion [49], allowing orbital tracking beyond the lifetime of *Gaia* and offering insight into the relation between radio and optical emission generated by SBHBs. Additionally, SBHB orbital tracking can yield precise binary mass measurements, or even a novel measurement of the Hubble constant [49].

### A. Gravitational waves

The SBHBs detectable by *Gaia* would be emitting GWs in the PTA frequency band. As a consistency check, we follow Ref. [49] and use the QLF to compute the corresponding stochastic GW background (GWB). For simplicity and in difference from Ref. [49], we assume that the SBHBs are driven together only by GW radiation and that  $f_{\text{Edd}} = 0.1$ . The resulting GWB falls a factor of a few below the current PTA limits, consistent with previous studies [e.g., [71]].

The most massive and nearby *Gaia*-detectable SBHBs have  $M \sim 10^{8.5} M_{\odot}$  and  $z \sim 0.01$  (Fig. 1). Such an SBHB, with a mass ratio of unity and an orbital period of less than 3 yr, could be resolved as an individual source with a  $\sim 13$ -yr PTA observation. Determination of the orbital parameters and location on the sky by *Gaia* could aid PTA detection.

### B. Caveats

Throughout we have assumed that only one SBH is bright and that the light centroid of the system moves a characteristic distance given by the orbital semimajor axis. Depending on the relative masses and luminosities of the two SBHBs, however, this distance can vary. The motion of the light centroid can be discerned from the difference

between the fixed center of mass of the binary and the center of light. Defining the Eddington-fraction ratio of the SBHBs as  $\xi \equiv f_{\text{Edd},1}/f_{\text{Edd},2} \leq 1$ , we find that the change in light centroid over an orbit is

$$\theta_{\text{orb}} = \frac{2a}{D_A(z)} \left( \frac{1}{1+q} - \frac{\xi}{1+\xi q} \right), \quad (4)$$

simplifying to our fiducial value,  $a/D_A(z)$ , when only one SBH in an equal mass binary is bright ( $\xi = 0$  and  $q = 1$ ). Orbital motion is undetectable when both SBHBs are accreting at the same fraction of Eddington. However, this is a finely tuned case disfavored by previous work [32,50]. If  $\xi \leq 1/3$ , then our adopted  $\theta_{\text{orb}}$  is reduced by less than a factor of 2.

Because the primary sources for SBHB identification with *Gaia* are nearby AGN, extended emission from a resolved nucleus could contribute to the optical centroid. The extent of this complication must be studied further, ideally for specific AGN candidates.

Another source of uncertainty lies in the assumption that an unknown fraction  $f_{\text{bin}}$  of AGN are triggered by SBHBs. Additionally, our calculation relies on the unknown rate at which SBHBs are driven to merger. We have only included orbital decay due to GW radiation, as this is a process that must occur. But gas accretion must also occur for the SBHBs to be optically bright. To test the effect of gas accretion on our results, we included a prescription for gas-driven orbital decay from Ref. [49]. Gas-driven decay does not affect our result when occurring at less than the Eddington rate. Furthermore, the binaries could stall before they make it to the small separations considered here, in that case our binary probability prescription is invalid and neither *Gaia* nor any other technique will find very compact SBHBs. However, detection of an SBHB with *Gaia* could rule out that possibility.

Since a detection of SBHBs would be the first of its kind, one may ask if the SNR cut that we adopt from [58], originally intended for astrometric planet detection, yields a higher false-positive rate than desired for such a task. Considering that there are only  $\sim 10^3$  bright nearby AGN for which this detection method could be employed (e.g., Fig. 1) and that the 50% detection rate is computed using a detection criterion that was shown by Ranalli *et al.* [58] to yield a  $\lesssim 10^{-4}$  false-positive rate, we view this as an acceptable minimum criterion for motivating the possibility of SBHB orbital tracking.

We finally note that the number of SBHBs with orbital separation larger than the end-of-mission precision and  $P_{\text{max}} \leq 20$  yr is large,  $\approx 440 f_{\text{bin}}$ . Such systems would move by an orbital separation that is resolvable by *Gaia* over its lifetime, but not necessarily resolved by the single-scan precision for each of *Gaia*'s  $\sim 70$  observations. While not offering a definitive detection of an SBHB, such anomalous

astrometric measurements of AGN light centroids should be flagged for further investigation.

#### IV. CONCLUSION

We have shown that a 10-yr *Gaia* mission has the capability to astrometrically track the orbital motion of  $\mathcal{O}(1)$  SBHBs in bright ( $m_V \lesssim 13$ ), nearby ( $z \lesssim 0.02$ ) AGN. The discovery of SBHB orbital motion over the next few years of the *Gaia* mission would open a new field of SBHB demography, generating an enormous boon for our understanding of the mutual growth of SBHBs and galaxies, evidence toward resolving the final-parsec problem, the prospect of sources of gravitational waves for PTAs, and a

new method for calibrating cosmological distances [49]. There is a strong incentive to analyze astrometric data of bright, nearby AGN from *Gaia* DR2 and onward for signatures of SBHB orbital motion.

#### ACKNOWLEDGMENTS

We thank the anonymous referees for their useful comments that improved the quality of this work. Financial support was provided from NASA through Einstein Postdoctoral Fellowship Grant No. PF6-170151 (DJD) and through the Black Hole Initiative which is funded by a grant from the John Templeton Foundation.

- 
- [1] M. A. C. Perryman, K. S. de Boer, G. Gilmore, E. Høg, M. G. Lattanzi, L. Lindegren, X. Luri, F. Mignard, O. Pace, and P. T. de Zeeuw, *Astron. Astrophys.* **369**, 339 (2001).
  - [2] T. Prusti, J. H. J. de Bruijne, A. G. A. Brown, A. Vallenari, C. Babusiaux, C. A. L. Bailer-Jones, U. Bastian, M. Biermann, D. W. Evans *et al.* (Gaia Collaboration), *Astron. Astrophys.* **595**, A1 (2016).
  - [3] A. G. A. Brown, A. Vallenari, T. Prusti, J. H. J. de Bruijne, C. Babusiaux, C. A. L. Bailer-Jones, M. Biermann, D. W. Evans, L. Eyer *et al.* (Gaia Collaboration), *Astron. Astrophys.* **616**, A1 (2018).
  - [4] L. Lindegren *et al.*, *Astron. Astrophys.* **616**, A2 (2018).
  - [5] V. V. Makarov, J. Frouard, C. T. Berghea, A. Rest, K. C. Chambers, N. Kaiser, R.-P. Kudritzki, and E. A. Magnier, *Astrophys. J. Lett.* **835**, L30 (2017).
  - [6] L. Petrov and Y. Y. Kovalev, *Mon. Not. R. Astron. Soc.* **471**, 3775 (2017).
  - [7] Y. Y. Kovalev, L. Petrov, and A. V. Plavin, *Astron. Astrophys.* **598**, L1 (2017).
  - [8] L. Petrov, Y. Y. Kovalev, and A. V. Plavin, *Mon. Not. R. Astron. Soc.* **482**, 3023 (2019).
  - [9] M. C. Begelman, R. D. Blandford, and M. J. Rees, *Nature (London)* **287**, 307 (1980).
  - [10] D. Merritt and M. Milosavljević, *Living Rev. Relativity* **8**, 8 (2005).
  - [11] P. Amaro-Seoane *et al.*, [arXiv:1702.00786](https://arxiv.org/abs/1702.00786).
  - [12] A. N. Lommen, *J. Phys. Conf. Ser.* **363**, 012029 (2012).
  - [13] A. Gould and H.-W. Rix, *Astrophys. J. Lett.* **532**, L29 (2000).
  - [14] P. J. Armitage and P. Natarajan, *Astrophys. J. Lett.* **567**, L9 (2002).
  - [15] A. I. MacFadyen and M. Milosavljević, *Astrophys. J.* **672**, 83 (2008).
  - [16] F. G. Goicovic, A. Sesana, J. Cuadra, and F. Stasyszyn, *Mon. Not. R. Astron. Soc.* **472**, 514 (2017).
  - [17] A. Gualandris, J. I. Read, W. Dehnen, and E. Bortolas, *Mon. Not. R. Astron. Soc.* **464**, 2301 (2017).
  - [18] Y. Tang, A. MacFadyen, and Z. Haiman, *Mon. Not. R. Astron. Soc.* **469**, 4258 (2017).
  - [19] Y. Shen and A. Loeb, *Astrophys. J.* **725**, 249 (2010).
  - [20] P. Tsalmantza, R. Decarli, M. Dotti, and D. W. Hogg, *Astrophys. J.* **738**, 20 (2011).
  - [21] T. Bogdanović, M. Eracleous, and S. Sigurdsson, *New Astron. Rev.* **53**, 113 (2009).
  - [22] M. Eracleous, T. A. Boroson, J. P. Halpern, and J. Liu, *Astrophys. J. Suppl. Ser.* **201**, 23 (2012).
  - [23] B. McKernan, K. E. S. Ford, B. Kocsis, and Z. Haiman, *Mon. Not. R. Astron. Soc.* **432**, 1468 (2013).
  - [24] R. Decarli, M. Dotti, M. Fumagalli, P. Tsalmantza, C. Montuori, E. Lusso, D. W. Hogg, and J. X. Prochaska, *Mon. Not. R. Astron. Soc.* **433**, 1492 (2013).
  - [25] Y. Shen, X. Liu, A. Loeb, and S. Tremaine, *Astrophys. J.* **775**, 49 (2013).
  - [26] X. Liu, Y. Shen, F. Bian, A. Loeb, and S. Tremaine, *Astrophys. J.* **789**, 140 (2014).
  - [27] J. Liu, M. Eracleous, and J. P. Halpern, *Astrophys. J.* **817**, 42 (2016).
  - [28] K. Nguyen, T. Bogdanović, J. C. Runnoe, M. Eracleous, S. Sigurdsson, and T. Boroson, *Astrophys. J.* **870**, 16 (2019).
  - [29] Z. Haiman, B. Kocsis, and K. Menou, *Astrophys. J.* **700**, 1952 (2009).
  - [30] D. J. D’Orazio, Z. Haiman, and A. MacFadyen, *Mon. Not. R. Astron. Soc.* **436**, 2997 (2013).
  - [31] D. J. D’Orazio, Z. Haiman, P. Duffell, B. D. Farris, and A. I. MacFadyen, *Mon. Not. R. Astron. Soc.* **452**, 2540 (2015).
  - [32] B. D. Farris, P. Duffell, A. I. MacFadyen, and Z. Haiman, *Astrophys. J.* **783**, 134 (2014).
  - [33] M. J. Graham, S. G. Djorgovski, D. Stern, A. J. Drake, A. A. Mahabal, C. Donalek, E. Glikman, S. Larson, and E. Christensen, *Mon. Not. R. Astron. Soc.* **453**, 1562 (2015).
  - [34] M. Charisi, I. Bartos, Z. Haiman, A. M. Price-Whelan, M. J. Graham, E. C. Bellm, R. R. Laher, and S. Márka, *Mon. Not. R. Astron. Soc.* **463**, 2145 (2016).
  - [35] T. Liu, S. Gezari, W. Burgett, K. Chambers, P. Draper, K. Hodapp, M. Huber, R.-P. Kudritzki, E. Magnier, N. Metcalfe, J. Tonry, R. Wainscoat, and C. Waters, *Astrophys. J.* **833**, 6 (2016).

- [36] D. J. D’Orazio and Z. Haiman, *Mon. Not. R. Astron. Soc.* **470**, 1198 (2017).
- [37] D. J. D’Orazio and R. Di Stefano, *Mon. Not. R. Astron. Soc.* **474**, 2975 (2018).
- [38] A. C. Gower, P. C. Gregory, W. G. Unruh, and J. B. Hutchings, *Astrophys. J.* **262**, 478 (1982).
- [39] N. Roos, J. S. Kaastra, and C. A. Hummel, *Astrophys. J.* **409**, 130 (1993).
- [40] D. Merritt and R. D. Ekers, *Science* **297**, 1310 (2002).
- [41] C. Zier and P. L. Biermann, *Astron. Astrophys.* **396**, 91 (2002).
- [42] G. E. Romero, L. Chajet, Z. Abraham, and J. H. Fan, *Astron. Astrophys.* **360**, 57 (2000).
- [43] E. Kun, K. É. Gabányi, M. Karouzos, S. Britzen, and L. Á. Gergely, *Mon. Not. R. Astron. Soc.* **445**, 1370 (2014).
- [44] E. Kun, S. Frey, K. É. Gabányi, S. Britzen, D. Cseh, and L. Á. Gergely, *Mon. Not. R. Astron. Soc.* **454**, 1290 (2015).
- [45] G. Kulkarni and A. Loeb, *Mon. Not. R. Astron. Soc.* **456**, 3964 (2016).
- [46] F. K. Liu, S. Li, and X. Chen, *Astrophys. J. Lett.* **706**, L133 (2009).
- [47] N. Stone and A. Loeb, *Mon. Not. R. Astron. Soc.* **412**, 75 (2011).
- [48] E. R. Coughlin, P. J. Armitage, C. Nixon, and M. C. Begelman, *Mon. Not. R. Astron. Soc.* **465**, 3840 (2017).
- [49] D. J. D’Orazio and A. Loeb, *Astrophys. J.* **863**, 185 (2018).
- [50] D. J. D’Orazio, Z. Haiman, and D. Schiminovich, *Nature (London)* **525**, 351 (2015).
- [51] C. M. Peters, G. T. Richards, A. D. Myers, M. A. Strauss, K. B. Schmidt, Ž. Ivezić, N. P. Ross, C. L. MacLeod, and R. Riegel, *Astrophys. J.* **811**, 95 (2015).
- [52] S. Jester, D. P. Schneider, G. T. Richards, R. F. Green, M. Schmidt, P. B. Hall, M. A. Strauss, D. E. Vanden Berk, C. Stoughton, J. E. Gunn, J. Brinkmann, S. M. Kent, J. A. Smith, D. L. Tucker, and B. Yanny, *Astron. J.* **130**, 873 (2005).
- [53] D. W. Evans *et al.*, *Astron. Astrophys.* **616**, A4 (2018).
- [54] S. Casertano, M. G. Lattanzi, and M. A. C. Perryman, *Astrophys. Space Sci.* **241**, 89 (1996); S. Casertano, M. G. Lattanzi, and M. A. C. Perryman, in *Future Possibilities for Astrometry in Space*, edited by M. A. C. Perryman and F. van Leeuwen, ESA Special Publication Vol. 379 (1995), pp. 47–54, <https://ui.adsabs.harvard.edu/abs/1995ESASP.379...47C>.
- [55] H.-H. Bernstein and U. Bastian, in *Future Possibilities for Astrometry in Space*, edited by M. A. C. Perryman and F. van Leeuwen, ESA Special Publication Vol. 379 (1995), p. 55, <https://ui.adsabs.harvard.edu/abs/1995ESASP.379...55B>.
- [56] S. Casertano, M. G. Lattanzi, A. Sozzetti, A. Spagna, S. Jancart, R. Morbidelli, R. Pannunzio, D. Pourbaix, and D. Queloz, *Astron. Astrophys.* **482**, 699 (2008).
- [57] M. Perryman, J. Hartman, G. Á. Bakos, and L. Lindegren, *Astrophys. J.* **797**, 14 (2014).
- [58] P. Ranalli, D. Hobbs, and L. Lindegren, *Astron. Astrophys.* **614**, A30 (2018).
- [59] P. F. Hopkins, G. T. Richards, and L. Hernquist, *Astrophys. J.* **654**, 731 (2007).
- [60] G. T. Richards, M. Lacy, L. J. Storrie-Lombardi, P. B. Hall, S. C. Gallagher, D. C. Hines, X. Fan, C. Papovich, D. E. Vanden Berk, G. B. Trammell, D. P. Schneider, M. Vestergaard, D. G. York, S. Jester, S. F. Anderson, T. Budavári, and A. S. Szalay, *Astrophys. J. Suppl. Ser.* **166**, 470 (2006).
- [61] G. Kauffmann and T. M. Heckman, *Mon. Not. R. Astron. Soc.* **397**, 135 (2009).
- [62] F. Shankar, D. H. Weinberg, and J. Miralda-Escudé, *Mon. Not. R. Astron. Soc.* **428**, 421 (2013).
- [63] D. W. Hogg, [arXiv:astro-ph/9905116](https://arxiv.org/abs/astro-ph/9905116).
- [64] P. Martini, [arXiv:astro-ph/0304009](https://arxiv.org/abs/astro-ph/0304009).
- [65] D. Hobbs *et al.*, [arXiv:1609.07325](https://arxiv.org/abs/1609.07325).
- [66] M.-P. Véron-Cetty and P. Véron, *Astron. Astrophys.* **518**, A10 (2010).
- [67] M. Charisi, Z. Haiman, D. Schiminovich, and D. J. D’Orazio, *Mon. Not. R. Astron. Soc.* **476**, 4617 (2018).
- [68] C. Jordi, M. Gebran, J. M. Carrasco, J. de Bruijne, H. Voss, C. Fabricius, J. Knude, A. Vallenari, R. Kohley, and A. Mora, *Astron. Astrophys.* **523**, A48 (2010).
- [69] C. L. MacLeod, Ž. Ivezić, B. Sesar, W. de Vries, C. S. Kochanek, B. C. Kelly, A. C. Becker, R. H. Lupton, P. B. Hall, G. T. Richards, S. F. Anderson, and D. P. Schneider, *Astrophys. J.* **753**, 106 (2012).
- [70] M. J. Graham, S. G. Djorgovski, D. Stern, E. Glikman, A. J. Drake, A. A. Mahabal, C. Donalek, S. Larson, and E. Christensen, *Nature (London)* **518**, 74 (2015).
- [71] L. Z. Kelley, L. Blecha, L. Hernquist, A. Sesana, and S. R. Taylor, *Mon. Not. R. Astron. Soc.* **471**, 4508 (2017).